

**A380 FLEXIBLE PAVEMENT EXPERIMENTAL PROGRAM : DATA ACQUISITION  
AND TREATMENT PROCESS, FIRST NUMERICAL SIMULATIONS AND  
MATERIAL TESTING**

By :

**J.PETITJEAN**

*STBA, 31 av du Maréchal Leclerc F 94381 Bonneuil sur Marne, France*

**C.FABRE**

*AIRBUS, 1 rond point M.Bellonte F 31707 Toulouse, France*

**J.M.BALAY**

*LCPC, route de Bouaye BP4129 F44341 Bouguenais, France*

**PRESENTED FOR THE 2002 FEDERAL AVIATION ADMINISTRATION AIRPORT  
TECHNOLOGY TRANSFER CONFERENCE**

05/02

## 1 ABSTRACT:

The paper describes several experimentations on flexible pavements at Toulouse Blagnac airport, tested with heavy aircraft landing gear simulator developed by Airbus : both static and fatigue tests.

The theoretical analyses of the static tests experimental results uses first a multi-layer linear elastic model (ALIZE), and in some cases a Finite Element modelling tool (CESAR – LCPC). The paper presents adjustments found between experimental measurements and calculations models for surface deflection and resilient strains for subgrade, untreated and bituminous materials.

The paper presents finally the fatigue experiment and some planned laboratory tests to analyse the results of this campaign.

## 2 PRESENTATION OF THE PROGRAM

The issue of pavement compatibility was considered by AIRBUS to be fundamental to the A380 program, especially as the current ACN/PCN method, was shown to have reached its limit of readability. In this general context, AIRBUS initiated in 1998 a very complete and ambitious experimental program, in partnership with the French Airport and Airforce Bases Engineering Department (STBA) and the French Laboratory for Civil Engineering (LCPC). This research program, named A380 Pavement Experimental Program (A380 PEP) was launched in June 1998.

Two targets were mainly assigned to the A380 PEP :

- to provide comparative experimental data sustaining AIRBUS A380 Landing Gear configuration selection process.
- to provide fundamental full-scale data for a better understanding of flexible pavement structures behavior against wide bodies loading cases, with special interest in the validation of the classical Linear Elastic Model and/or the development of other models (FEM).

Ultimately, the A380 PEP will participate in the development of a new pavement design method, based on the multi-layered linear elastic model addressing flexible pavement design, which is usually considered to be more efficient than the current CBR method.

The A380 PEP includes two main parts, the first one (nowadays in course of completion) dealing with the flexible pavements (flexible PEP), and the second one (2001-2003) dealing with the rigid pavements (rigid PEP). This paper only presents the flexible phase of the program, divided in two successive stages (as the future rigid phase): the static stage and the fatigue stage.

### 2.1 *Flexible experimental pavements design*

The site selected for building the specimen pavement was on Toulouse Blagnac airport as extension of an existing taxiway. The test pavement was 165m long, 30m wide. Each test section was 35m long separated from the next one by a 5m long “neutral zone”.

Four sections of flexible pavement structures were designed according to the French method (i) for four different subgrade categories: CBR 4, 6, 10, 15. The test taxiway was built to the current design standard for a B747-400 (10 000 coverages). Structures made of the same materials and the same thickness for bituminous layers (Bituminous Concrete 8cm, Bituminous Gravel

2\*12cm), the subbase layer had a variable thickness depending on the Subgrade and made of Humidified Reconstituted Crushed Gravel. Three out of four subgrades were found on site (CBR 15, 10, and 6). The weakest subgrade, CBR 4, was reconstituted with imported material.

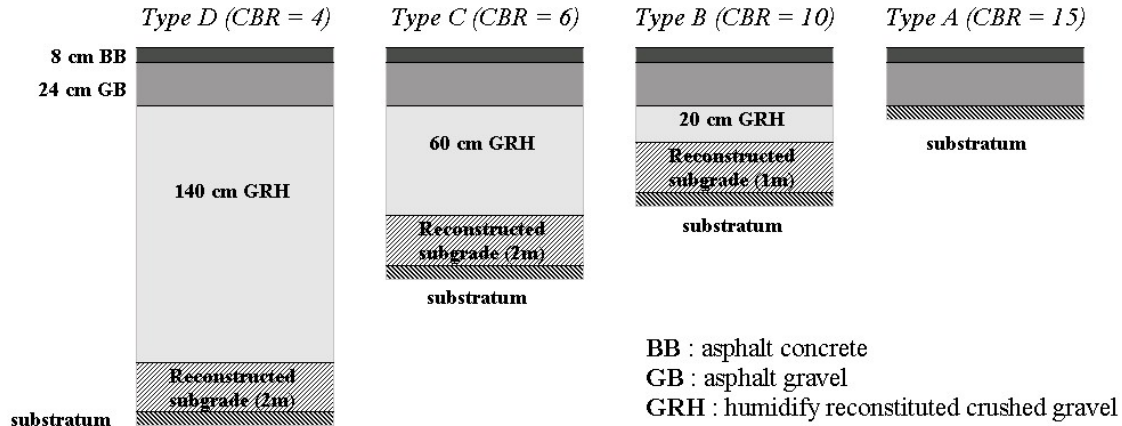


**Figure 1.** PEP structures

## 2.2 Pavements instrumentation

Each specimen pavement section was instrumented on one side only due to symmetry of the tested aircraft configurations. Four main resilient strain sensors layers were installed, namely: at the Top of the Subgrade, at the Bottom of the Subbase (GRH), at the Top of the Subbase (GRH), and at the Bottom of the Bituminous Gravel (GB).

A total of some 250 sensors were imbedded in the four sections, along transversal profiles, to provide redundancy.

The transversal separation interval between sensors was larger for the deepest layers where the wheel grouping effect was expected to induce a larger area of loading influence (Subgrade and Bottom Subbase interval was 60cm)

In the upper layers, the stress diffusion pattern is sharper and restricted to a smaller area around the wheels, therefore there was a need for closer sensors (Top Subbase and Bituminous Gravel interval is 15cm).

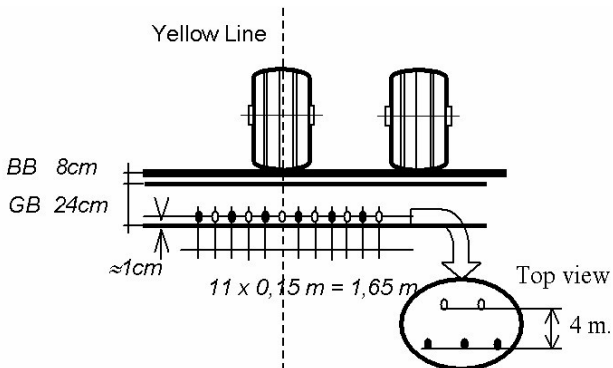


**Figure2.** Alternated horizontal strain gauges location transversal profile on GB base

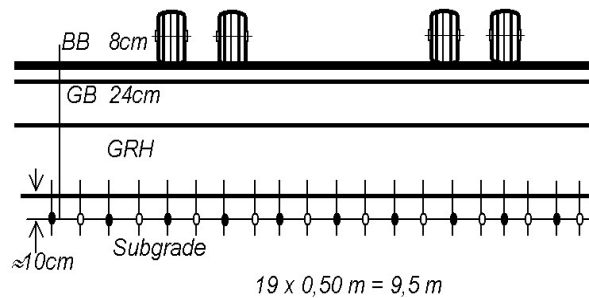


**Figure 3.** Alternated vertical strain gauges location transversal profile on top subgrade

In addition to the existing resilient strain gauges , specific permanent deformation sensors were installed in 1999 for the specific fatigue testing campaign.

These sensors locating at the GB/GRH interface and GRH/subgrade interface are anchored at 6 m depth, in the subgrade, and are intended to measure individual layer permanent strain in the two weakest test sections (CBR 6 and 4).

### 2.3 The simulation vehicle

In order to adequately represent wide bodies Landing Gear (L/G) loading cases, a simulation vehicle was designed. A full-scale vehicle was selected because of the non-linearity of weak subgrades to the loading. The vehicle concept is modular.

One module figures out one bogie; it can be either a 4 to 6-wheels module or a basic diabolo (2-wheels). On each module, the geometry is variable for the track and tandem distances.

Modules can be assembled according to various dimensions in 2 to 5 modules arrangements depending on the aircraft L/G which is represented.

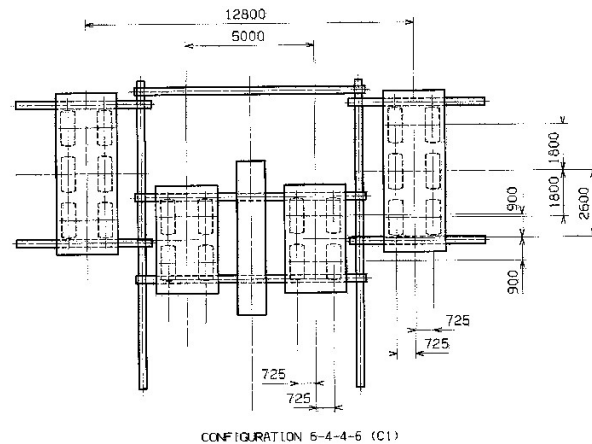
Each module is individually loaded with applicable steel plates. A dual cantilever system distributes the weight among the wheels on 6-wheelers so as to ensure uniform load distribution ; when 4-wheelers are used, a forefront driving diabolo with minimal loading reacts as a cantilever limitation with the same purpose without influencing significantly the instrumentation.

It has been checked that the vehicle behaves as a real aircraft on the pavement and can carry up to each specific aircraft MTOW (maximum take off weight) corrected by the most aft CG (center gear) MLG (main landing gear) position. Loading is made with a crane.

The vehicle features an autonomous power and hydraulic supply capable of controlling its trajectory and speed. Nominal taxiing speed is 2km/h.



**Figure 4.** Simulation vehicle



A340 tires are used whatever the aircraft L/G configuration is tested. Tire pressures are set so as to reproduce the actual contact area and contact pressure of the original (or developed ) tire.

The opportunity to circulate real aircraft on specimen pavement enabled to validate both the vehicle mechanical concept and the tire pressure setting procedure. Especially by comparing aircraft and vehicle B747 configurations, resilient deformations proved to correlate very well with some 5% difference (piling up measuring error, temperature effect, and speed effect).

### 3 QUASI STATIC TESTS

#### 3.1 Tests procedures

The static test campaign began on 3<sup>rd</sup> November 1998 to finish on 28<sup>th</sup> April 1999, and have tested 15 vehicle configurations, as 3 real aircraft. Before each configuration, a reference load was used (module of two wheels loaded each one with 30 tons) for the following reasons :

A more or less long space of time separates necessarily the strain gauge recordings relative to two load configurations. During this time, the parameters of structural behavior of the pavement in general change under the effects of the variations of the environmental conditions (temperatures, hygrometry, or evolution of the structural rigidity...). The establishment of objective comparisons between the various configurations of load will thus require a first harmonization called the “temporal harmonization” (coefficient Cht). It is based on the analysis of the strains measured by the whole gauges, for the reference load.

A second type of harmonization is necessary as explained now. For a layer of a given structure, the localization of the maximum strain varies with the load configuration. The strain gauge revealing the maximum value could thus be different from one configuration to another. But the response to a given load of several gauges of a given type is not single: it is sensitive to metrological conditions, to the characteristics of its insertion in materials, and also to the natural heterogeneity of instrumented material. The establishment of objective comparisons between configurations will also require a second harmonization called the “space harmonization” (coefficient Chs). It is based too on the analysis of the maximum strains measured by the whole gauges of a given type, for the same reference load.

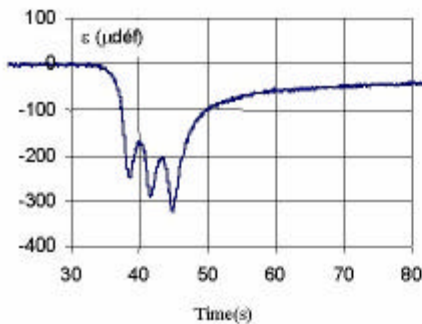


**Fig 5a :** Transversal Strain (Gauge 1T03)

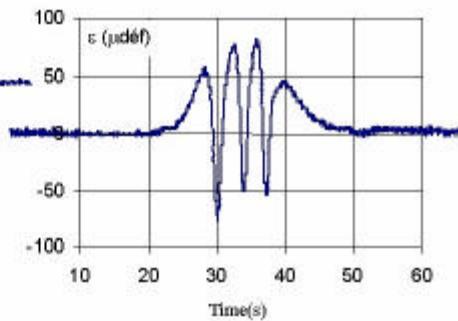


**Fig 5b :** Longitudinal Strain (Gauge 1L03)

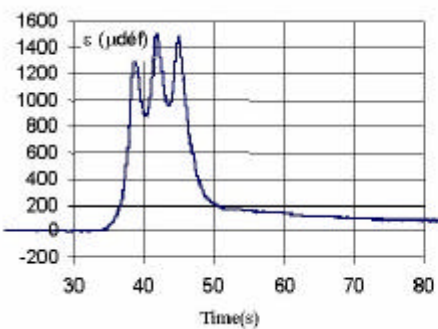


**Fig 5c :** Vertical Strain on top of GRH  
(Gauge 1H09)

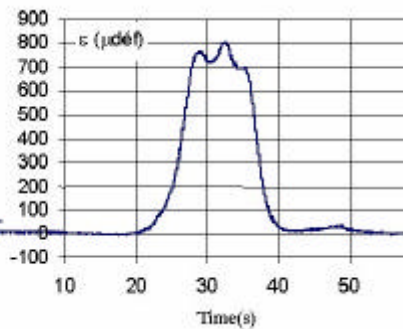


**Fig 5d :** Vertical Strain on base of GRH  
(Gauge 1B06)

**Figures 5.** Extensometric measures, standard signals (before double harmonization). Example for C22 configuration (6x6), structure D (03-03-1999, 13h56 min)

For the spatial as for the temporal harmonization, it is observed that the coefficients  $C_h$ s and  $C_{ht}$  obtained express corrections to be applied to the rough strains, which are often higher than several tens of percent. This high order of magnitude justifies the place which is given in our analysis, to the operations of harmonization of the strain measurement, and secondly invites right now to consider with prudence the comparisons between the tested configurations, which should be based exclusively on the corrected extensometric measurements. Keeping constant the tire load, it is clear that geometrical changes of the bogie of a few centimeters exert variations on the internal strains in the pavement, which are quite lower than the corrections of harmonization of the measurements attached to each configuration.

### 3.2 Data analyses

#### 3.2.1 Selection of the most interesting configurations for the analysis

On the totality of the configurations tested, 8 configurations are selected, taking into account the two following criteria:

- The values of the characteristic bogie parameters (wheel base, wheel track, number wheels and load per wheel) of these 8 configurations must correctly frame the values of these same parameters on the 20 configurations tested on the whole;
- The gauges recording of the selected configurations must not raise any interrogation, and the whole test parameters during measurement have to be correctly controlled.

**Table 1.** 8 configurations selection for detailed exploitation.

Tested Configuration		Load/wheel (kN)	Tire Press (MPa)	Track (cm)	Wheel base (cm)	L1 (cm)	L2 (cm)	L3 (cm)
CB1	4-4-4-4	232	0.88	112	147	1100	384	307
CB2	6-6	239	1.53	140	145	1097	/	/
C1	6-4-4-6	260	1.34	145	180	1280	500	260
C7	4-6-6-4	260	1.34	145	180	1280	500	280
C5H	4-6-6-4	260	1.34	135	180	1280	500	280
C8	4-6-2-6-4	261	1.34	145	180	1280	500	280
C17	4-4-4	311	1.65	140-118-140	198	1068	/	76
C22	6-6	286 239	1.48 1.53	135 - 140	170 - 145	600	/	/

*L1: spacing between Wing Landing Gear (WLG) axes*

*L2: spacing between Center Landing Gear (CLG) axes*

*L3: X spacing between WLG and CLG axes*

The results of the strains measurements presented before are the subject of a final synthesis intended to facilitate work of numerical simulation that will follow. This synthesis is established while considering the not-interaction between them of the various bogies composing a given configuration, like that is exposed before.

We shall retain, for a bogie of characteristics given (number of wheels, geometry, weight per wheel and inflation pressure), a single value of the maximum strain created by this bogie in a given structure and a given layer of material, independently of the global geometry of the configuration to which it belongs. One admitted to consider as the same bogie, several bogies whose wheel-base varies from a value lower or equal to 10 cm, all other characteristics unchanged.

6 bogies of different characteristics have been identified, 3 bogies with 4 wheels noted in the continuation bogie 4a, 4b and 4c, and 3 bogies with 6 wheels noted bogie 6a, 6b and 6c.

**Table 2.** configurations selection for numerical modeling.

Bogie n°	bogie type	weight/wheel (kN)	Tire press. Load (MPa)	Track (m)	Wheel base (m)
4a	4 wheels	260	1.34	1,35/1.45	1.80
4b	4 wheels	232	0.88	1.12	1.47
4c	4 wheels	316	1.34	1.4/1.18/1.4	1.98
6a	6 wheels	239	1.53	1.40	1.45
6b	6 wheels	260	1.34	1.45	1.80
6c	6 wheels	286	1.48	1.35/1.45/1.35	1.70

### 3.2.2 Multi layer elastic model calibration

The aim of this part of the study is to evaluate the possibilities of numerical simulation to determine the maximum strains measured in the PEP structures during static tests. This is done firstly by mean of the classical linear elastic multi-layers model (l.e.m model) of road mechanics. We used Alizé software of LCPC, which is an application of the solutions proposed by Burmister to this problem. The hypothesis of the simulation are those of Burmister's model.

The adjustment of the Alizé model is done with the values of the modulus of rigidity of the various layers of materials and the subgrades for the structures B, C and D (structure A was not analyzed due to building defects). The criterion of appreciation of the adjustments is the agreement between the maximum measured strains and strains calculated by the model. Some rules have been adopted to range the value of modulus (tests temperature for asphalt materials modulus...)

The results are the following:

**Table 3:** Simulation of the structures B, C and D for the six bogies resulting from the analysis of the static tests. Structures adjusted with Alizé software (*Poisson coefficient = 0,35 for all materials*)

Structure B CBR 10		Structure C CBR 6		Structure D CBR 4	
Material and thickness	Young modulus (MPa)	Material and thickness	Young modulus (MPa)	Material and thickness	Young modulus (MPa)
BB 8 cm	3 000	BB 8 cm	3 000	BB 8 cm	6 000
GB 24 cm	5 000	GB 24 cm	5 000	GB 24 cm	8 000
GRH 20 cm	80	GRH 60 cm	110	GRH 70 cm	100
Subgrade 1 m	80	Subgrade 1 m	50	GRH 70 cm	70
substratum	15 000	Subgrade 1 m	150	Subgrade 2 m	60
		Substratum	15 000	substratum	15 000

### Comments on the adjustments obtained

- Quality of simulation : the differences between measurements and calculations show an adjustment very close to the theoretical model
  - for the GRH, the differences vary between -14% and +18%. 78% of the calculated deformations present a lower deviation less than 10% of measurements;
  - for the subgrade, the differences vary between -16% and +16%. 72% of the calculated deformations present a lower deviation less than 10% of measurements.

The values, which precede, characterize from our point of view a very correct adjustment of the model. By way of comparison, adjustments of this quality are rarely obtained with the experiments carried out on the LCPC's fatigue test track. Experimental difficulties encountered on

tests campaign, in particular the precision of spatial and temporal harmonization, come to reinforce this opinion on the quality of the corrections .

- Modules of bituminous materials: the corrections lead for the structures B and C with the values of modules 3 000 MPa for the BB and 5 000 MPa for GB. These values appear in agreement with the conditions of temperature (16°C approximately) and the speed of the simulation vehicle (approximately 2 km/h). The values obtained for the structure D, 6 000 MPa and 8 000 MPa respectively, appear also coherent, taking into account the reference temperature which is 12°C approximately for this structure.
- Modules of the GRH: the module obtained for GRH of structure B (20 cm), structure C (60 cm) and of the higher part of structure D (70 cm) varies between 80 MPa and 110 MPa. These relatively low values are explained by the significant thickness of the bituminous layers (32 cm) which may attenuate the average constraints supported by the untreated low register, by thus attenuating the nonlinear character of its behavior. On the lower layer of GRH of the structure D (70 cm), the value of modulus of 70 MPa is to be connected in fact to the module of the subgrade support of 60 MPa. Our experiment in road structures leads in general to observe a low discontinuity of modulus in this part of the structure near the interface between the subgrade and the untreated granular sub-base.
- Modules of the subgrade: the values of modules obtained for the subgrades of the three structures seems to be enough surprising, because they badly reflect the values of the respective CBR presented by these three materials at construction. It is difficult however to stop an opinion on these results, as long as the laboratory tests on the three subgrades will not have identified their law of behavior, different moreover according to the subgrade. The average pressures at the top of the subgrade of the structure B are normally higher than at the top of the subgrade of the structure D, because the thickness of very different GRH. The non linear model of Boyce for unbound road materials, which establishes a strengthener of material with the average pressure, would lead to values of module appreciably higher for the subgrade of the structure B than for that of structure D. We have to observe however that this nonlinear model is especially validated for the untreated graded aggregates. The laws of behavior for the subgrades are very varied. One should not exclude that another form of dependence between the average pressure, the shear stress and rigidity can justify the values of modules obtained for the three subgrades, in spite of their initial values of CBR.

### **Conclusions on the capacities of the multi-layered linear elastic model**

- For the three structures B, C and D resulting from this adjustment, the classical multi-layered linear elastic model (Alizé-LCPC software) allows a rather precise determination of the maximum deformations generated at the top of the subgrade and the top of the GRH by six isolated standard bogies (three bogies 4 wheels and three bogies 6 wheels).
- The questions concerning the influence on the strains in pavements, of the geometrical and weight characteristics of the bogies have partly justified the static tests of the flexible PEP. The experimental results alone do not bring the awaited complete quantitative answers, because of the obvious complexity of the experimental process, and the low precision of the operations of spatial and temporal harmonization which it was essential to apply. One will find in the multi-layer linear elastic model the sufficiently precise quantitative answers to these questions, only as regards the maximum strains in the untreated materials and in the subgrade



- The classical model appears on the other hand unsuited, to obtain a realistic description of the strains measured at the base of the bituminous layer, in particular the bending strains under the tires which control the possible fatigue damage of this material.

This limitation applies to:

- The absolute values of the maximum strains.
- The ranking of the maximum strains created by the six bogies.
- And the orientation of the maximum bending tensile strains, longitudinal according to the model and transversal according to measurements.

This limitation is due to visco elasticity of bituminous materials not considered by the multi-layered linear elastic model.

### 3.2.3 First viscoelastic simulation of PEP test

We tried to improve the simulation by Alizé software of the maximum strain measured, in particular as regards the direction of the maximum tensile strain, by two approaches:

- By modifying the distribution of contact pressures between the tires and the pavement surface. These attempts appeared unable to improve to a significant degree the quality of simulations. It is observed that the deformations at the base of the bituminous base are in fact rather not very sensitive to the form of the distribution of the pressures under the tire, because of the strong thickness of the bituminous cover.
- By taking account the thermo-visco-elastic behavior of bituminous materials. A simplified and exploratory study was undertaken in this direction, with the use this time of the finite element code of calculation César-LCPC, module CVCR. The module CVCR makes it possible to simulate the behavior of a multi-layer pavement loaded by a moving load, and comprising one or more layers of materials with visco elastic behavior. The assumptions of this modeling were as follows:
  - modeled structure: structure C
  - Single thermo-visco-elastic law of behavior for the BB and GB: model of Huet and Sayegh <sup>(ii)</sup> consisting in two parallel branches. The first branch has a parabolic spring and two absorbers corresponding to instantaneous and delayed elasticity of the material. The second branch has a single spring corresponding to the static or long-term behavior of material.

$$E^*(\omega, \theta) = E^\circ + \frac{(E^\infty - E^\circ)}{1 + \delta(\omega\tau)^{-k} + (i\omega\tau)^{-h}}$$

with :

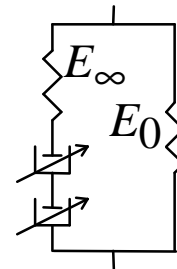
$E_\infty$  : instantaneous elastic modulus,

$E^\circ$  : delayed elastic modulus,

$\delta$  : not dimensionnal coefficient  $> 0$ ,

$t(q)$  : decreasing function of temperature,

$k, h$  : exponents of the creep laws of the parabolic spring ( $1 > h > k > 0$ ),



- Loading of the model: bogie 6b moving at the speed 2.0 km/h, surface of contact with the pavement consisting in a rectangular form (side 0.44 m, uniform pressure applied 1.34 MPa).

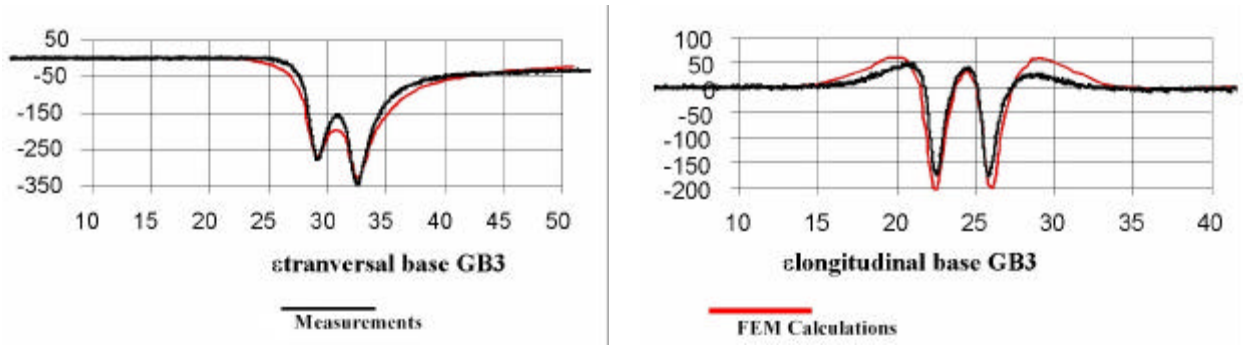


**Figure 6:** Modeling with the thermo-visco-elastic Huet & Sayegh's Model (FEM César-Lcpc software): comparison between measurements and theoretical results for the 4 wheels bogie of C17 configuration, structure C

It must be underlined that this first modeling have to be consider from a strictly qualitatively angle, in absence any laboratory test which should permit a precise description of the visco-elastic law of bituminous PEP materials.

These first attempt with CVCR is very encouraging, and it clearly indicates that the taking into account of the thermo-visco-elasticity of the bituminous material is likely to contribute to a simulation much more realistic of the deformations generated by the slow aeronautical loads in flexible pavement.

## 4 FATIGUE TESTS

### 4.1 Fatigue configuration selection

For the fatigue tests (5000 passes of the simulator), the simulator is equipped with four different bogies

**Table 4:** the 4 tested bogies during the fatigue phase

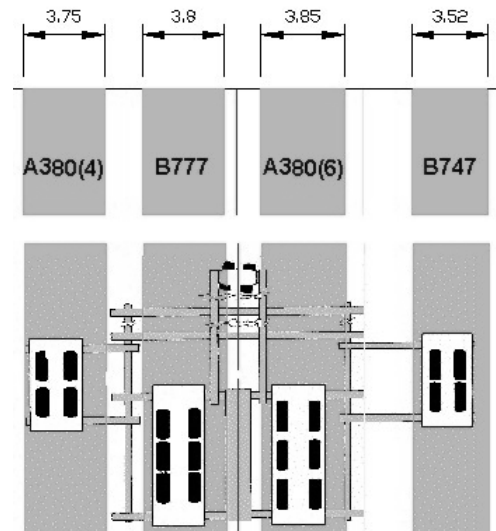
	4 wheels	6 wheels
230 kN/wheel	B747	B777
280 kN/wheel	A380	A380

**Figure 7:** Fatigue simulation vehicle configuration

(4 and 6 wheels) as shown in the following table

These 4 bogies were set up together on the simulation vehicle, to be run simultaneously, with the same climatic and wandering conditions as during the fatigue phase period.

The important assumption during the experimental phase was that the interaction of the 4 bogies could be neglected for most of it, even despite the wandering condition. This assumption is based on the results from PEP static phase, which showed that the resilient strains induced within the bandwidth of a bogie was unaffected by the neighboring bogies.



The figure shows the configuration, which was used for the test (A380-4W, B777-6W, A380-6W, and B747-4W) as well as the bandwidth for each bogie, including the  $\pm 1$  m wandering condition, which was adopted during the fatigue campaign.

#### 4.2 Tests procedures

The campaign started in October 1999 and ended in July 2000 and was composed of 2 phases.

- The first phase consisted in running the simulation vehicle 2500 times forwards and backwards (5 000 passes) with wandering of  $\pm 1$  m about a central position. To achieve this goal 9 longitudinal lanes (named A to I), 22 cm width, were painted side by side along the pavement and used as a guide. The number of passes over the different strips was chosen as below, with lane E as the mean position.

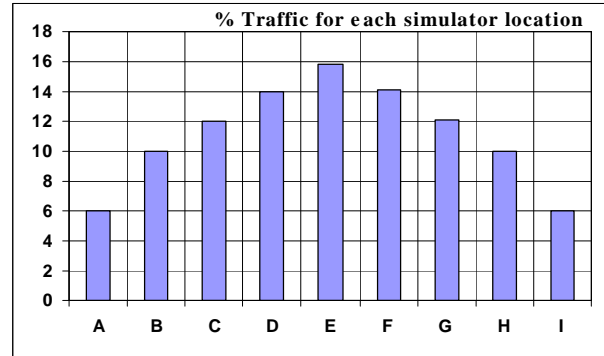


**Figure 8:** Percentage of traffic on each lane

A randomizing process of lane trafficking have been adopted to avoid repetitive coverage of the pavement when its temperature was at a maximum or minimum.

- It was decided in the second phase to run 500 more F/B movements (1 000 passes) without wandering and to wait for the periods of the day when the pavement temperature was at its maximum.

The objective of that phase was to try accelerate both the rutting of the bituminous layer and the possible rutting of the GRH and reconstituted soil layers.

In order to keep the main deformation pattern obtained around position E unchanged, it was decided for this second phase to run the simulation vehicle in position I.

#### 4.3 Pavement Condition Follow-up

The evolution of PEP pavements during the fatigue campaign was followed through different variables measured with different tools and different modalities. The table below summarizes the auscultation campaign.

**Table 5:** Pavement condition follow up

Measurement	Tool	Modality
Pavement surface deformation	Topography with external reference	Every 1000 passes
	Straight edge along three predefined transversal profiles for each structure (B,C,D)	Every 100 passes
Calculation of STBA Service Index (IS)	Pallas tool = laser measurement over the all pavement surface	Beginning and end of the fatigue campaign
Assessment of the state condition of interlayer interface	Geotechnical radar	Beginning and end of the fatigue campaign
Global assessment of the pavement structural condition	Bearing plate measurements following with STBA procedure	Beginning and end of the fatigue campaign

A further difficulty should be noted. That was the difficulty to characterise in detail the mechanical state of the pavement at the end of the static phase, which is expected to be transversally heterogeneous, since the coverage was unevenly distributed during that phase. In particular, the area along the yellow reference line of static tests was more trafficked than any other part of the

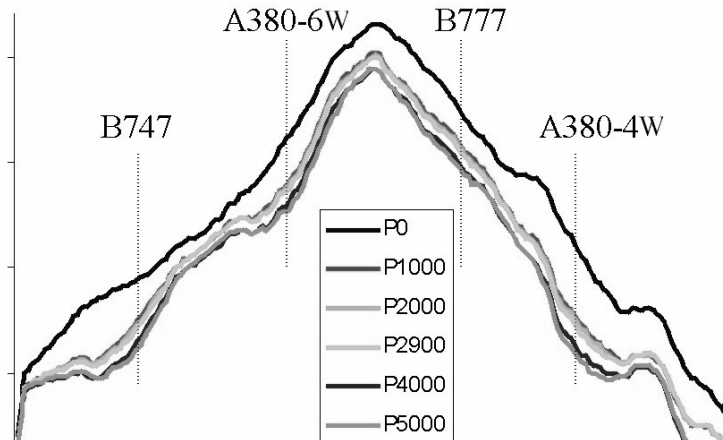


**Figure 9:** Example of cross section typical survey

pavement. That means that the four different bogies cannot be compared with the absolute values, but only with the relative evolution of each parameter from the beginning of the fatigue tests.

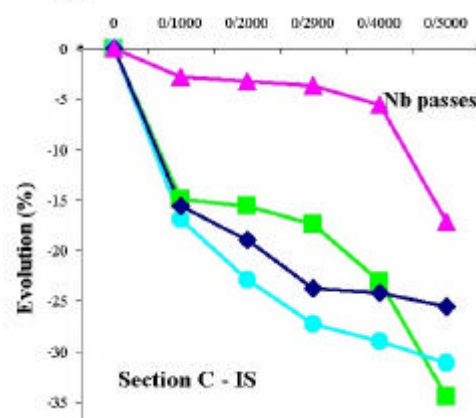
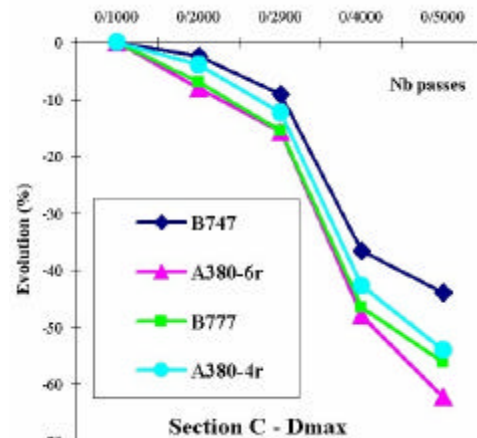
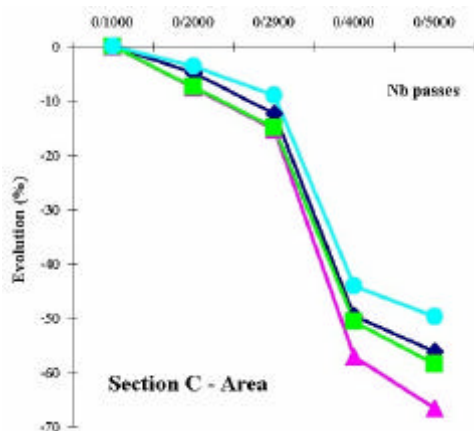
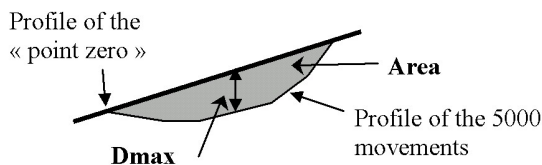
The topographical survey shows a significant generalized settlement on all platforms between the « point zero » ( $P_0$ ) and the first 1000 movements ( $P_{1000}$ ). The average settlement on each platform is:

- Platform B: 4 mm,
- Platform C: 16 mm,
- Platform D: 13 mm.

This shows that the consolidation phase has kept on after the static tests. This conforms to what happens in reality, as it is well known that the consolidation stage takes place one or two years of the pavement life.

Special parameters were monitored : the evolution of the maximum of the depression and the evolution of the area of the depression compare to the « point zero » (called respectively *Dmax* and *Area*).

**Figures 10:** Example of parameters relative evolution (section C)



The first conclusions of the monitoring by current tools (Service Index and topographical survey) of the pavement during the fatigue campaign are the following:

- there is no severe distresses (cracks...) of the pavement after 5000 passes .
- no direct comparison is possible because the starting “level” of the trafficked pavement is not homogenous for all the strips,
- And finally no absolute classification is possible between the different landing gear configurations (for any sections).

Other studies are so necessary to analyse the fatigue campaign.

#### 4.4 Final observations and materials samplings

Samplings from the soils, as well as from the crushed gravel and bituminous mix were taken out from the structures, B, C and D after the end of the experiment.

The aim is to characterize the evolution of these materials along the whole PEP experimentation, comparing their final and initial mechanical performances whether the samples were taken respectively from the traffic lanes or outside them.

Transversal trenches dug to the natural soil were realized in B, C and D structures. The observation of their vertical sides could help to evaluate the structural state of the pavements at the end of fatigue tests (presence of reflective cracking at the base of the layers ?) and also to analyze the distribution of the total rutting measured at the surface of the pavement, between the different layers of materials . The trenches also allowed final stiffness (EV<sub>2</sub>), by performing some usual bearing plate tests at their base. The results of these in situ plate tests are presented in table 6. They reveal an increase of stiffness of soil B and particularly soil D during the experiment.

**Table 6:** Evolution of soils stiffness during the experiment (in situ tests)

Soil	After construction		At end of experiment	
	Water content	Mean Modulus EV <sub>2</sub>	Water content	Mean Modulus EV <sub>2</sub>
<b>B</b>	8% to 11%	75 MPa ( $\sigma = 5.2$ MPa)	7.6 %	88 MPa ( $\sigma = 15.1$ MPa)
<b>C</b>	17% to 19%	33 MPa ( $\sigma = 3.4$ MPa)	16.6 %	36 MPa ( $\sigma = 2.7$ MPa)
<b>D</b>	25.6% to 30.9 %	20.3 MPa ( $\sigma = 3.4$ MPa)	26.9 % to 28.9 %	38 MPa

The tables 7 and 8 below show the planned lab tests for the unbound and bituminous materials.

**Table 7:** Planned tests for unbound materials

Material	Planned tests
Soil from structure B	Identification ; Moisture
Soil from structure C & Soil from structure D	Characterisation ; Moisture ;CBR RLT* with adapted procedure to PEP condition
Crushed gravel	Identification ;Moisture RLT with the usual procedure for road condition (LRPC-T) RLT with procedure adapted to the PEP condition

\*RLT = Repeated Load Triaxial Test

**Table 8:** Planned tests for bituminous materials

Materials	Binder extraction Grading curve Binder content	Void content	Complex modulus	Fatigue testing	Rutting**
<b>Bottom of GB</b>					
<i>Outside wheel-path</i>	✓	✓	✓	✓	
<i>Under wheel-path</i>		✓	✓	✓	
<b>Top of GB</b>					
<i>Outside wheel-path</i>		✓	✓		✓
<i>Under wheel-path</i>		✓	✓		
<b>Bituminous wear course</b>					
<i>Outside wheel-path</i>	✓	✓	✓		✓
<i>Inside wheel-path</i>		✓	✓		

Triaxial tests were only performed on soils C and D and not on soil B, because of its very coarse grading (0/60 mm). For soils C and D, resilient behavior was found to be practically linear elastic, with a very slight anisotropy ( $E_v/E_h < 2$ ). The variations with water content of the elastic moduli issued from triaxial test are presented in table 9. The comparison with the in situ stiffness (cf. table 6) shows that field conditions are difficult to reproduce exactly in laboratory tests.

**Table 9:** Values of elastic moduli from triaxial tests

		In situ values			
<b>Soil C</b>	<b>W(%°)</b>	15.6%	16.4%	17.9%	16.6%
	<b>E (MPa)</b>	94	60	44	$E_v = 36 > \text{MPa}$
<b>Soil D</b>	<b>W (%°)</b>	20.6%	29.4%	31.4%	29%
	<b>E (MPa)</b>	91	62	59	$E_v = 38 \text{ MPa}$

Concerning the characterization of granular unbound materials with repeated load triaxial tests, it has been found that their resilient behavior is correctly described by the anisotropic Boyce model. A poor resistance to permanent strains for these materials has also been observed from triaxial tests

The main results (at this day) of laboratory study of bituminous materials are synthesized in tables 10 and 11.

**Table 10:** Void content measurement in bituminous materials

	Structure B – A380 6 wheels			Structure D – A380 6 wheels		
	No traf- fic	Traffic with wandering	Traffic without wandering	No traf- fic	Traffic with wandering	Traffic without wandering
Wearing course (bitu- minous concrete)	2.2%	2.1%	1%	2.4%	1.2%	1.3%
Top of GB	4.4%	2.4%	7.1%	5.9%	3.7%	9.4%
Bottom of GB	5.6%	6.8%	3.5%	5.7%	5.9%	4.8%

**Table 11:** summary of first complex modulus and fatigue tests

Structure – material	Complex modulus (15°C, 10Hz)	Fatigue testing
Structure C - bottom of GB – outside wheel path	10 300 MPa	$\epsilon_6 = 73 \mu\text{strain}$ voids : 9.2%
Structure B - bottom of GB – highest trafficked lane	14 900 MPa	$\epsilon_6 = 89 \mu\text{strain}$ voids : 3.2%
Structure C – wearing course (bituminous concrete) - outside wheel path	10 950 MPa	
Structure C - top of GB – outside wheel path	13 170 MPa	

These results show that the first effects of traffic on bituminous layer are clearly the densification of the bituminous concrete and the GB for the two structures B and D. This densification leads to an increase of moduli and fatigue characteristics of bituminous materials. This absence of fatigue damage of the GB in the trafficked area is confirmed by in situ observations of the material done in the trenches (no apparent cracking).

The laboratory studies aiming to the complete determination of mechanical properties of the materials are still continuing, mainly for improving the conditions of modeling of the pavement behavior during the fatigue stage. For instance, additional fatigue tests at high strain levels, representative of aeronautical loading conditions (300  $\mu$ strains, 10 000 load cycles) are programmed.

## 5 CONCLUSION

As a first result of this experimentation, a very complete database has been obtained. It permits first objective comparisons between the effects of the different tested configurations, and it secondly gathers useful data for the developpement of a new aeronautical rational design method for flexible pavements. The classical multi-layer elastic model appears to be suitable for the static simulation of untreated materials and soils, but not for the asphalt materials. For these materials, the thermo-visco-elastic constitutive law of Huet & Sayegh is believed to provide a more useful tool, and the first simulations are very encouraging. The in situ and laboratory tests performed on pavement materials have shown a densification with the traffic of soils and bituminous materials, leading to an increase of their stiffness (and also of the fatigue performances for asphalt concrete). The analysis of fatigue phase results and complementary laboratory tests are still continuing, and will be presented in a future article.

---

## BIBLIOGRAPHY

<sup>i</sup> **Ministère des Transports, DGAC, SBA, STBA.** “Instruction sur le dimensionnement des chaussées d’aérodromes et la détermination des charges admissibles”, volume 1. 1983.

<sup>ii</sup> **HUET,C,** “Etude par une méthode d’impédance du comportement viscoélastique des matériaux hydrocarbonés”, thèse de Docteur Ingénieur, Faculté des Sciences de Paris, 1963.